

CrystEngComm

Accepted Manuscript

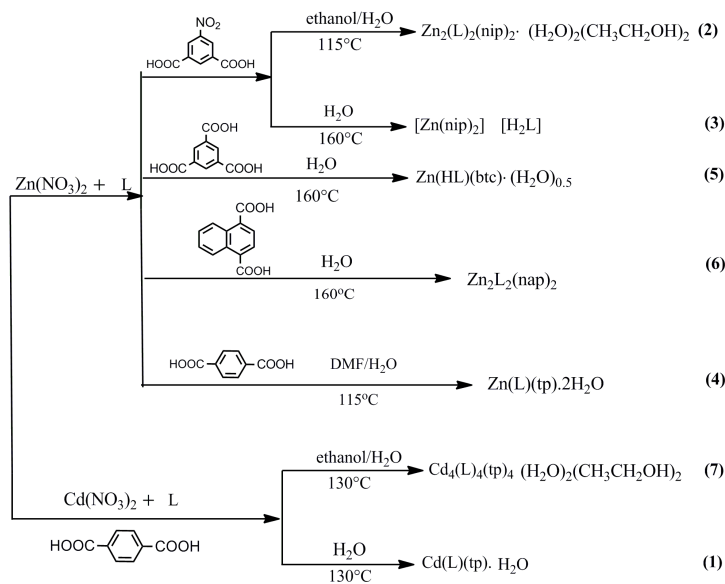


This is an *Accepted Manuscript*, which has been through the Royal Society of Chemistry peer review process and has been accepted for publication.

Accepted Manuscripts are published online shortly after acceptance, before technical editing, formatting and proof reading. Using this free service, authors can make their results available to the community, in citable form, before we publish the edited article. We will replace this *Accepted Manuscript* with the edited and formatted *Advance Article* as soon as it is available.

You can find more information about *Accepted Manuscripts* in the [Information for Authors](#).

Please note that technical editing may introduce minor changes to the text and/or graphics, which may alter content. The journal's standard [Terms & Conditions](#) and the [Ethical guidelines](#) still apply. In no event shall the Royal Society of Chemistry be held responsible for any errors or omissions in this *Accepted Manuscript* or any consequences arising from the use of any information it contains.



With the different synthesis condition, a series of compounds based on L ligands are obtained. The resulting compounds, **1-7**, show different structural features, involving interpenetrating, interlocked, puncturing, and pillared-layered framework.

Construction and Modulation of Structural Diversity in acylamide-MOFs

Shu-yun Huang, Jian-qiang Li, Shu-juan Liu,* Yang Ning, Li-na Meng, Jin-yuan Li, Ming-biao Luo, and Feng Luo*

College of Biology, Chemistry and Material Science, East China Institute of Technology, Nanchang, Jiangxi, China Fax: 86 0794 8258320; Tel: 86 0794 8258320; E-mail: ecitluofeng@163.com

ABSTRACT: A new N-donor ligand, N¹,N⁴-di(pyridin-4-yl)naphthalene-1,4-dicarboxamide (L) has been designed and applied to generate seven new acylamide-MOFs, namely, Cd(L)(tp)(**1**), Cd(L)(tp)(H₂O).(H₂O)₃.(CH₃CH₂OH)₃(**2**), Zn(L)(nip)(**3**), [Zn(nip)₂][H₂L](**4**), Zn(HL)(btc).(H₂O)_{0.5}(**5**), Zn(L)(nap)(**6**), Zn(L)(ip).(H₂O)₂.(CH₃CH₂OH)(**7**) (H₂tp=terephthalic acid, H₂nip=5-nitroisophthalic acid, H₂nap=naphthalene-1,4-dicarboxylic acid, H₃btc=benzene-1,3,5-tricarboxylic acid, H₂ip=isophthalic acid). **1** presents a rare 4-connected **sra** framework with 8-fold interpenetration in the [4+4] manner. Similar reaction conditions except for different reaction temperature and solvent as employed in **1** produced compound **2**, which shows a 2D net with two-fold interpenetration in the parallel fashion. Compound **3** and compound **4** are also synthesized with the same materials, but different solvent and reaction temperature, then **3** owns a 2D two-fold interpenetrating net in the parallel fashion and **4** is a 1D chain, but presents a 3D supramolecular net. In **5**, the 2D layer constructed by the Zn ions and btc³⁻ ligands, and the L ligand single protonated acts as the ornamental, but playing a puncture role. **6** is a 3D layer-pillared framework with α -Po topology and three-fold interpenetration, where Zn ions combine with the nap²⁻ ligands to form the 2D layer, and the L ligands act as the pillars. **7** also presents a 2D net. Moreover, thermogravimetric and fluorescence of some compounds has been explored.

Introduction

Over the past few years, metal-organic frameworks (MOFs) or coordination polymers have received a wide range of attention in the field of crystal engineering, not only because of their enormous varieties of interesting structural topologies, but also due to their promising application as functionalized materials.¹⁻⁵ The growth and design of MOFs is highly influenced by factors such as the structural characteristics of the organic ligand, the coordination nature of the metal ion, the metal-ligand ratio, the reaction condition, and other possible influences, which provides a possible approach to control the assembly of metal-organic frameworks.⁶⁻¹⁰ For the organic ligands, we can design the coordination site or the conformation to construct the desire MOFs.¹¹ Theoretically, the

compounds containing a same ligand exist an infinite number, but in fact, we has not yet obtained so much.

On the other hand, it is sagacious that constructing desired MOF must, in principle, reply on the choice of proper organic ligands. At present, the acylamide ligands is extensively used to prepare topological and functional MOFs, mainly dependent on the unique coordination and supramolecule-directing function.¹²⁻¹³ As far as we know, the N¹,N⁴-di(pyridin-4-yl)naphthalene-1,4-dicarboxamide (L) ligand has never been applied to design MOFs until this work. Acting as a kind of naphthalene carboxamide, it is promising in medicine, optics.¹⁴⁻¹⁶ There are a lot of properties worth researching. Therefore, to design the MOFs containing the L ligand is highly significant. Herein, with L ligands, we obtained seven novel acylamide-MOFs, namely, Cd(L)(tp)(**1**), Cd(L)(tp)(H₂O).(H₂O)₃.(CH₃CH₂OH)₃(**2**), Zn(L)(nip)(**3**), [Zn(nip)₂][H₂L](**4**), Zn(HL)(btc).(H₂O)_{0.5}(**5**), Zn(L)(nap)(**6**), Zn(L)(ip).(H₂O)₂.(CH₃CH₂OH)(**7**), (H₂tp=terephthalic acid, H₂nip= 5-nitroisophthalic acid, H₂nap=naphthalene-1,4-dicarboxylic acid, H₃btc=benzene-1,3,5-tricarboxylic acid, H₂ip=isophthalic acid) .

Experimental Section

Materials and Methods. The N¹,N⁴-di(pyridin-4-yl)naphthalene-1,4-dicarboxamide was prepared by the reported method.¹⁷ All other chemicals were obtained from commercial sources and used as received.

Physical Measurements. Thermogravimetric analyses (TGA) were carried out on METTLER TOLEDO TGA850 instrument in the temperature range of 25–400 °C under nitrogen atmosphere (flow rate of 50 mL min⁻¹) at a heating rate of 5 °C min⁻¹. Elemental analysis for C, H and N was performed on a Perkin-Elmer 240 analyzer. Steady-state photoluminescence spectra were measured on a SHIMADZU RF-5301PC spectro-Fluorophotometer.

Synthesis of Cd(L)(tp)(1**) and Cd(L)(tp)(H₂O).(H₂O)₃.(CH₃CH₂OH)₃(**2**).** Hydrothermal reaction was performed by using Cd(NO₃)₂.6H₂O (0.1 mmol), L (0.1mmol), and terephthalic acid (0.1 mmol) as raw materials , H₂O (8ml) as solvent under 130°C for 72 h, which produced colorless crystals of **1**. The colourless crystals are obtained in the yield of 13%, based on Cd for **1**. While ethanol (8ml) and H₂O (2ml) as solvent under 130 °C for 72 h, colorless crystals of **2** were obtained. The colourless crystals are obtained in the yield of 73%, based on Cd for **2**. Element analysis (%) of **2**: calcd: C 56.65, H 4.75, N 5.74; found: C 56.56, H 4.84, N 5.70.

Synthesis of Zn(L)(nip)(3**), [Zn(nip)₂][H₂L](**4**).** Hydrothermal reaction was performed by using Zn(NO₃)₂.6H₂O (0.1 mmol), L (0.1mmol), and 5-nitroisophthalic acid (0.2 mmol) as raw materials , H₂O (2ml) as solvent under 115 °C for 50 h, which produced colorless crystals of **3**. The colourless crystals are obtained in the yield of 17%, based on Zn for **3**. The same raw materials under 130°C

for 72 h produce colorless crystals of **4**. The colourless crystals are obtained in the yield of 77%, based on Zn for **4**. The phase purity of **4** is confirmed by both EA and XRD studies (Figure S1). Element analysis (%) of **4**: calcd: C 59.18, H 2.48, N 8.63; found: C 59.26, H 2.44, N 8.60.

Synthesis of Zn(HL)(btc).(H₂O)_{0.5}(5). Hydrothermal reaction was performed by using Zn(NO₃)₂.6H₂O (0.1 mmol), L (0.1mmol), and benzene-1,3,5-tricarboxylic acid (0.1 mmol) as raw materials, DMF(3ml), H₂O (1ml) as solvent under 115°C for 72 h, which produced colorless crystals of **5**. The colourless crystals are obtained in the yield of 75%, based on Zn for **5**. The phase purity of **5** is confirmed by both EA and XRD studies (Figure S2). Element analysis (%) of **5**: calcd: C 63.87, H 2.75, N 7.27; found: C 63.77, H 2.74, N 7.20.

Synthesis of [Zn(L)(nap)](6). Hydrothermal reaction was performed by using Zn(NO₃)₂.6H₂O (0.1 mmol), L (0.1mmol), and naphthalene-1,4-dicarboxylic acid (0.1 mmol) as raw materials, H₂O (8ml) as solvent under 160°C for 72 h, which produced colorless crystals of **6**. The colourless crystals are obtained in the yield of 78%, based on Zn for **6**. The phase purity of **6** is confirmed by both EA and XRD studies (Figure S3). Element analysis (%) of **6**: calcd: C 68.80, H 2.89, N 7.29; found: C 68.76, H 2.94, N 7.37.

Synthesis of [Zn(L)(ip)].(H₂O)₂.(CH₃CH₂OH)(7). Hydrothermal reaction was performed by using Zn(NO₃)₂.6H₂O (0.1 mmol), L (0.1mmol), and isophthalic acid (0.1 mmol) as raw materials, ethanol(4ml), H₂O (1ml) as solvent under 130°C for 72 h, which produced crystals of **7**. The colourless crystals are obtained in the yield of 71%, based on Zn for **7**. The phase purity of **7** is confirmed by both EA and XRD studies (Figure S4). Element analysis (%) of **7**: calcd: C 63.05, H 3.78, N 7.00; found: C 63.11, H 3.84, N 6.99.

Single-Crystal X-ray Diffraction. X-ray single-crystal structural data of **1–7** were collected on a Bruker Smart-CCD diffractometer equipped with a normal focus, 2.4 kW sealed tube X-ray source with graphite monochromated MoK α radiation ($\lambda = 0.71073 \text{ \AA}$) operating at 50 kV and 30 mA. The SAINT program was used for integration of diffraction profiles and absorption correction was made with the SADABS program. All the structures were solved by SIR 92 and refined by full matrix least-squares method using SHELXL 97. All the non-hydrogen atoms were refined anisotropically, and all the hydrogen atoms were fixed by HFIX and placed in ideal positions. All calculations were carried out using SHELXL 97, PLATON, and WinGX system, Ver 1.70.01. All crystallographic and structure refinement data of **1–7** are summarized in Table 1. CCDC number is 982327, 982328, 897889, 897890, 897891, 982329, 897888 for compounds **1-7**, respectively.

Table 1. Crystallographic and Structure Refinement Parameters for **1–7**.

Compounds	1	2	3	4	5	6	7

Formula	C ₄₀ H ₂₀ N ₄ O ₆ Cd	C ₄₆ H ₄₆ N ₄ O ₁₃ Cd	C ₄₀ H ₁₉ N ₅ O ₈ Zn	C ₄₈ H ₂₄ N ₆ O ₁₄ Zn	C ₄₁ H ₂₁ N ₄ O _{8.5} Zn	C ₄₄ H ₂₂ N ₄ O ₆ Zn	C ₄₂ H ₃₀ N ₄ O ₉ Zn
Mr	765.02	975.29	763.02	974.15	771.04	768.08	800.12
crystal system	monoclinic	Triclinic	Orthorhombic	Monoclinic	Monoclinic	Monoclinic	Triclinic
space group	<i>P2₁/c</i>	<i>P-1</i>	<i>Pbca</i>	<i>P2₁/c</i>	<i>P2₁/c</i>	<i>P2₁/c</i>	<i>P-1</i>
a (Å)	11.4377(5)	10.7918(4)	27.665(11)	15.0919(5)	11.8446(2)	8.5394(7)	9.9223(2)
b (Å)	10.9909(4)	22.0438(9)	21.903(7)	14.1967(5)	16.2081(2)	17.9536(16)	14.9699(3)
c (Å)	23.6256(10)	29.3454(11)	29.854(9)	18.1636(6)	15.5426(2)	14.6460(10)	21.0207(4)
α (deg)	90	78.661(2)	90	90	90	90	77.3650(10)
β (deg)	101.327(2)	81.342(2)	90	97.9410(10)	116.3730(10)	118.3440(10)	81.0100(10)
γ (deg)	90	83.766(3)	90	90	90	90	82.3770(10)
V (Å ³)	2912.1(2)	6744.3(4)	18090(11)	2719.3(2)	2673.29(7)	1978.24(4)	2993.54(10)
Z	4	2	8	4	4	4	1
D _{calc} (mg/m ⁻³)	1.562	1.306	1.416	1.526	1.615	1.581	0.145
F(0 0 0)	1376	2664	7872	1284	1328	956	120
R _{int}	0.0421	0.0797	0.1122	0.0309	0.0349	0.0238	1.053
GOF on F ²	1.210	1.059	0.977	1.066	1.070	1.083	1.053
R1 ^a [I>2σ(I)]	0.0736	0.0548	0.0766	0.0319	0.0357	0.0378	0.0644
ωR2 ^b (all data)	0.1815	0.1537	0.2179	0.0770	0.0850	0.1011	0.2334

Results and Discussion

Crystal structure description

Cd(L)(tp)(1). The single crystal X-ray diffraction reveals that polymer **1** crystallizes in monoclinic, *P2₁/c* space group. In **1**, each Cd(II) ion is six-coordinated with four oxygen atoms from two tp²⁻ ligands and two pyridine nitrogen atoms of two L ligands, creating a disordered octahedron geometry (Figure 1a). The tp²⁻ ligands take the μ₂:η¹:η¹:η¹ coordination mode, connecting to two Cd ions, which result in a 1D fold-like chain. Then, the L ligands taking the *trans* configuration (*trans* means that the two acylamide N-H groups of L ligand are in the same side and the dihedral angle between the naphthalene ring and the pyridine ring is 58.25°, 17.87° respectively) take bridge mode to join the adjacent 1D fold-like chains together through Cd-N bonds, ultimately resulting in a 3D framework with 1D hexagonal channels (Figure 1b), where π-π contacts occur between the pyridine rings of L ligands (the distance of centroid-to-centroid is 3.699 Å). Topologically, by considering each Cd(II) ion as one 4-connecting node, the 3D framework can be rationalized as a 4-connected **sra** nets with 4²6³8 topological symbol (Figure 1c). Notably, every four identical **sra** nets interpenetrate each other to form a 4-fold interpenetration, then resulting in the overall 8-fold interpenetration in the [4+4] mode (Figure 1d). As far as we know, in literatures, the **sra** net is common, but such net with higher interpenetrating number more than four is rare.¹⁸ Moreover, in spite of this 8-fold interpenetration, **1** also possess considerable voids, calculated by PLATON,

giving 324.1 \AA^3 (equal to 11.1% of the cell volume).

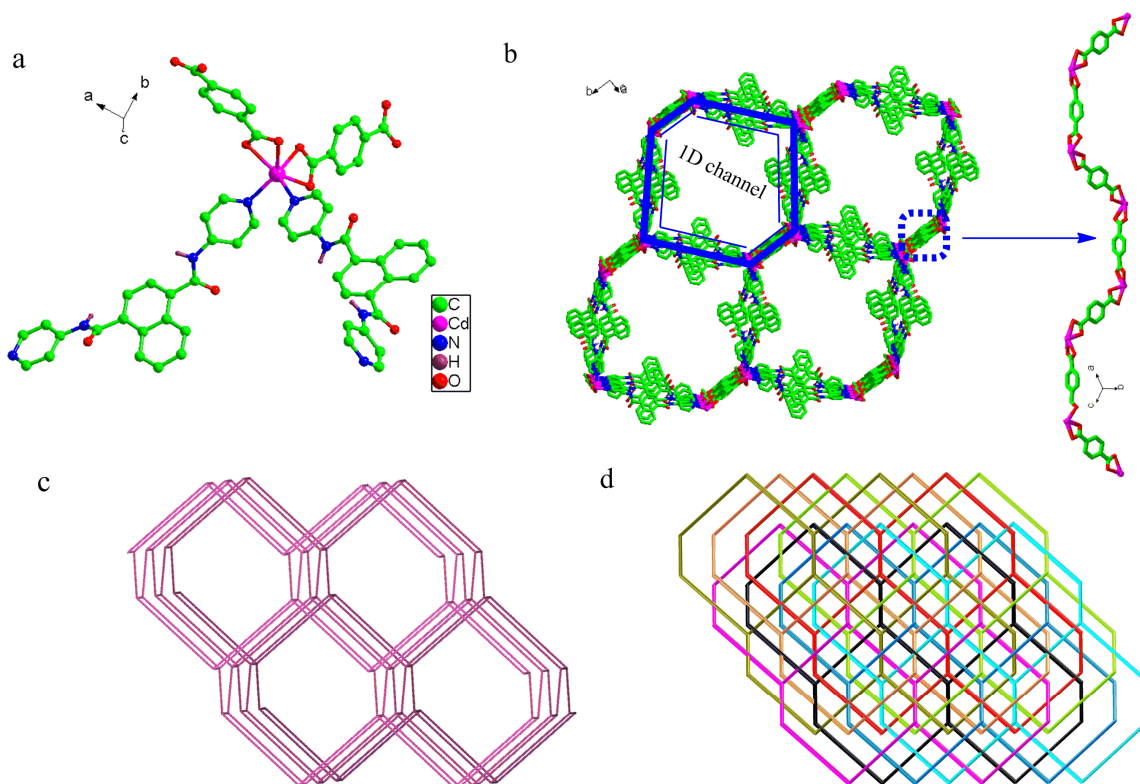


Figure 1. Structure of Cd(L)(tp) (**1**). (a) Coordination environment surrounding Cd(II) ion. (b) The 3D framework with 1D hexagonal channels and the 1D fold line chains. (c) The 3D 4-connected simplified nets of **1**. (d) The 8-fold (4+4) interpenetrated net of **1**.

Cd(L)(tp)(H₂O).(H₂O)₃.(CH₃CH₂OH)₃(2**).** The same materials as compound **1** but different solvent obtain compound **2**, which is with a complete different structure, a 2D wave-like layer (Figure 2b). It crystallizes in the triclinic *P*-1 space group. In **2**, there are four crystallographic independent Cd ions, which are all seven-coordinated with four oxygen atoms from two tp²⁻ ligands, two nitrogens from the pyridine group of two L ligands, and one oxygen from H₂O (Figure 2a). The L ligands take the same coordination mode as observed in compound **1** but different configuration of *anti* fashion (*anti* means that the two acylamide N-H groups are in the opposite side of L ligand), while the dihedral angle between the naphthalene ring and the pyridine ring is 67.83°, 17.34° respectively, which link with Cd ions to form a 1D line-shaped chain. After that, the 1D chains joined by the tp²⁻ ligands construct a 2D layer. Interestingly, in **1** and **2**, both tp²⁻ ligands and L ligands hold the same coordination mode, but the whole framework of them is throughly different, which mainly due to the existence of the additional coordinated oxygens from H₂O molecule observed in **2**. Notably, two independent 2D layers interlocked each other to finish a 2D 2-fold

parallel interpenetrated enlaced framework (Figure 2c), where there are seven kinds of hydrogen bonds, N15...H15M...O23 (2.868Å, 143.67°) between the L ligands, N3...H3M...O6(2.742Å, 164.63°), N7...H7M...O7(2.953Å, 169.37°), N6...H6M...O8(2.831Å, 151.54°), N10...H10M...O9(2.970Å, 166.59°), N11...H11M...O10(2.874Å, 168.77°), N14...H14M...O12(2.784Å, 148.28°) between L ligands and tp^{2-} ligands, which stabilize the interlocked framework. Calculated void space using PLATON was found to be 1804.1 Å³ (26.7% total of cell volume), indicative of potential porous material of **2**.

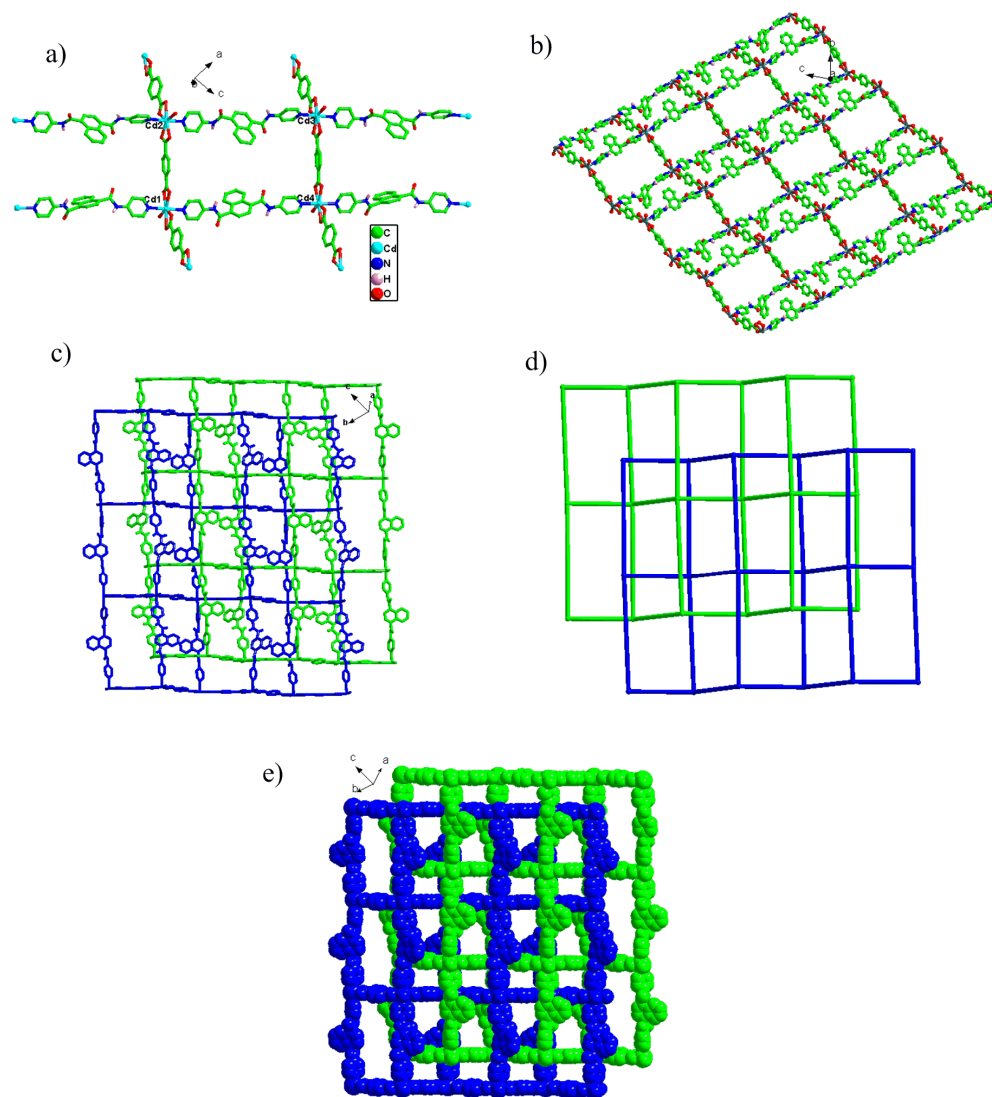


Figure 2. Structure of **2**. (a) The unit cell of **2**. (b) The 2D layer of **2**. (c) The 2D enlaced structure. (d) The simplified 4-connected 2D 2-fold interpenetrated enlaced framework of **2**. (e) The stacking framework of **2**.

Structure of [Zn(L)(nip)](3). As show in Figure 3a, in the unit cell of **3**, there are three

crystallographic independent Zn(II) ions, which are all with the same coordination mode. Each Zn connects to two oxygens from two different nip^{2-} ligands and two nitrogen from two different L ligands (the dihedral angle between the naphthalene ring and the pyridine ring is 68.37° , 21.27° respectively), giving a tetrahedral geometry. And the adjacent Zn ions share a nip^{2-} ligand. The L ligands and the nip^{2-} ligands both take a bidentate coordination mode. Both *trans* and *anti* configurations of L ligands are observed in **3**. Through L and nip^{2-} ligands these Zn(II) ions are combined together to construct a 2D wave-like layer (Figure 3b). And two 2D layers parallel interpenetrate in a interlocked fashion to give a interesting 2D twine structure (Figure 3c), which are further stabilized by two kinds of hydrogen bond between the L ligands and the nip^{2-} ligands, $\text{N12}\dots\text{H12}\dots\text{O2}$ (2.776\AA , 146.68°) and $\text{N2}\dots\text{H2}\dots\text{O10}$ (2.848\AA , 144.07°) respectively. Calculated void space using PLATON was found to be 2574.9\AA^3 (14.2% total of cell volume).

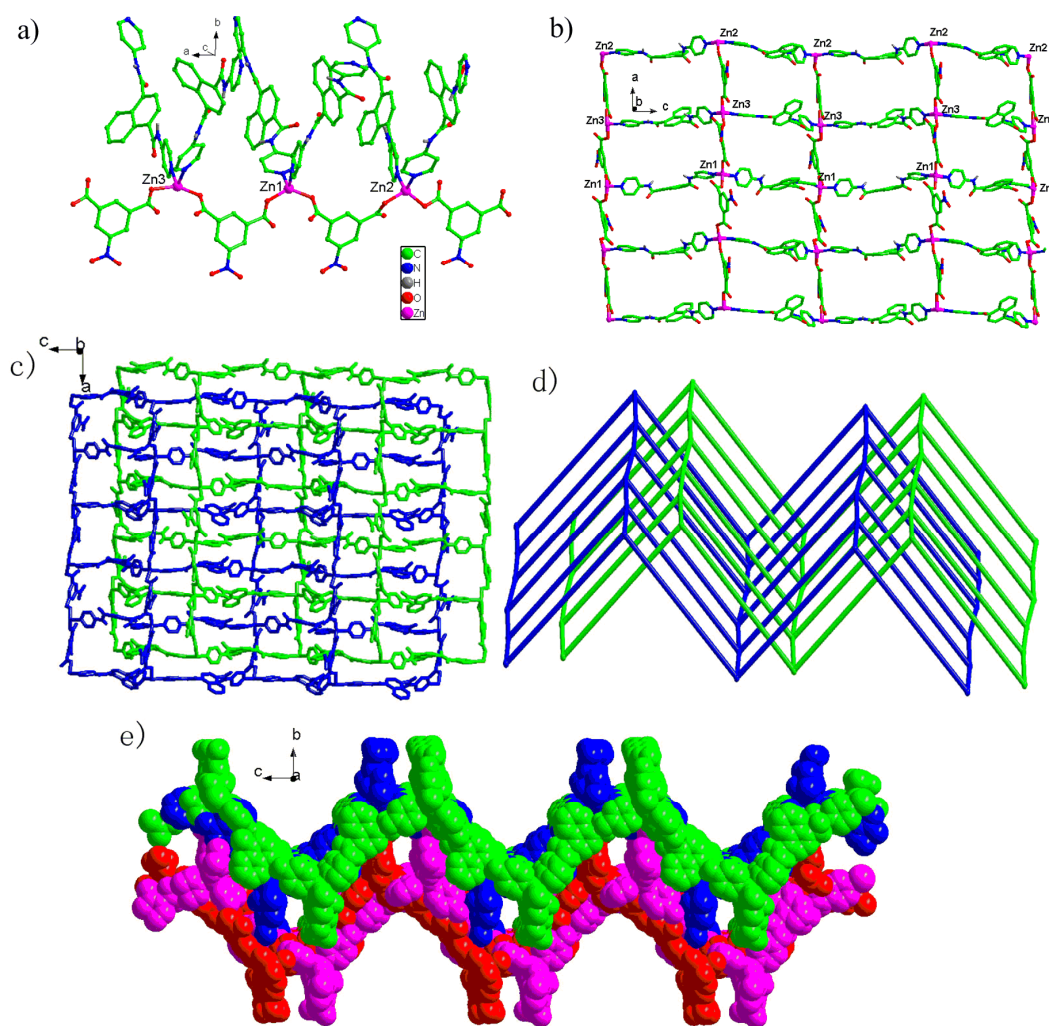


Figure 3. Structure of Zn(L)(nip) (**3**). (a) The unit cell of **3**. (b) The 2D wave-like layer of **3**. (c) The 2D enlaced structure. (d) the simplified enlaced framework of **3**. (e) The stacking framework of **3**.

Structure of $[\text{Zn}(\text{nip})_2][(\text{H}_2\text{L})](4)$. In **4**, as presented in Figure 4a, the unit cell contains one Zn(II) ion, four nip^{2-} ligands, and one $[\text{H}_2\text{L}]^{2+}$ unit, indicating an anion-cation compound and full protonation of L ligand. Each Zn is in a tetrahedral coordination sphere, and is surrounded by four nip^{2-} ligands as O-donors. Notably, the L ligands are doubly protonated to maintain the charge balance and the dihedral angle between the naphthalene ring and the pyridine ring is 73.14° , 64.62° respectively. The nip^{2-} ligands take a bidentate coordination mode connecting to two Zn ions. As shown in Figure 4b, along the *a* direction, two nip^{2-} ligands link with two Zn ions to form a sixteen-membered ring, then the rings combine with each other in a decussation way to form a 1D chain. Additionally, the N...H...O hydrogen bonds lying in the nip^{2-} ligands and the L ligands combine the L ligands and the 1D chains together to construct a 3D supermolecular framework $\{\text{N1...H1M...O4}(2.849\text{\AA}, 166.44^\circ)$, $\text{N2...H2M...O10}(2.865\text{\AA}, 170.43^\circ)$, $\text{N3...H3M...O7}(2.659\text{\AA}, 169.84^\circ)$, $\text{N4...H4M...O1}(2.615\text{\AA}, 157.54^\circ)$ respectively}, where the 1D chains stack in a regular arrangement, and the L ligands seem as filler (Figure 4c).

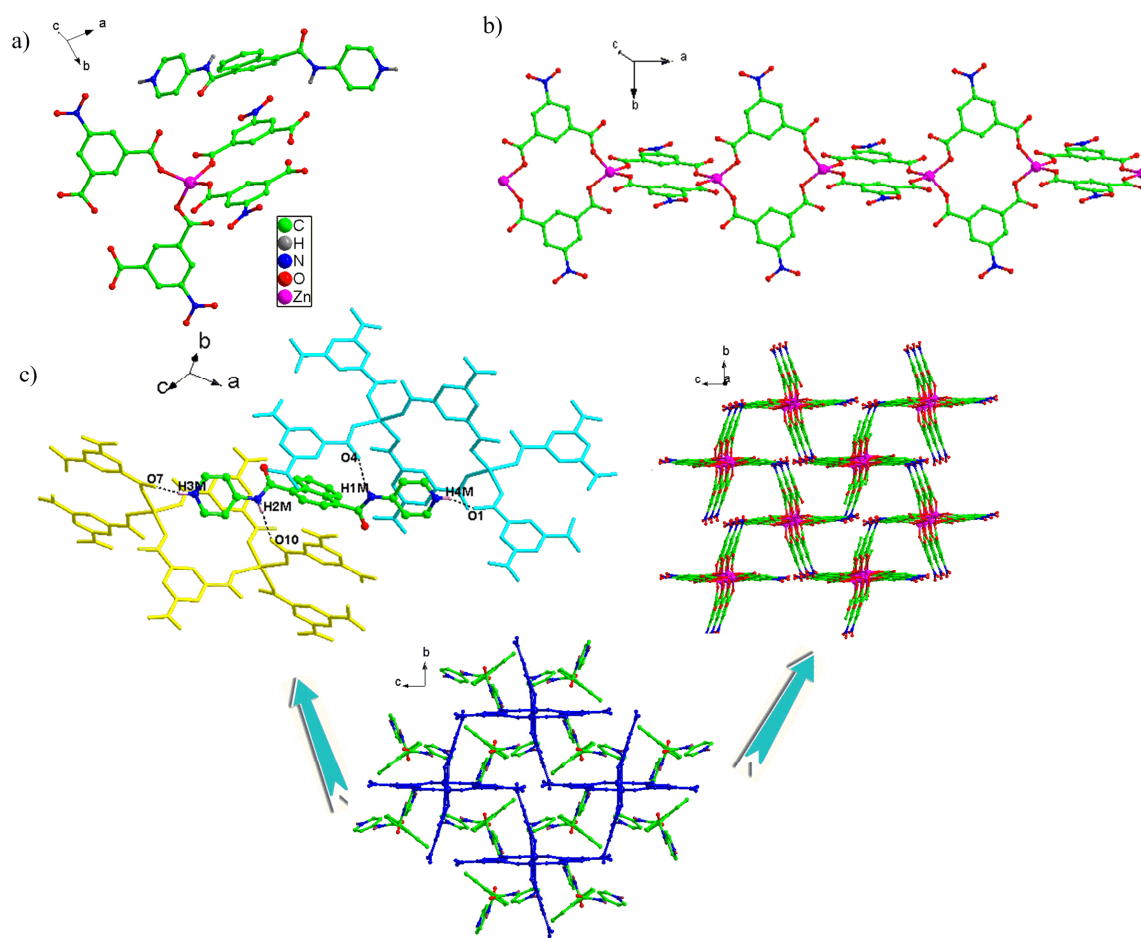


Figure 4. Structure of $[\text{Zn}(\text{nip})_2][(\text{H}_2\text{L})](4)$. (a) The unit cell of **4**. (b) The 1D cross-chain of **4**. (c) The details of filling framework of **4**.

Structure of $\text{Zn}(\text{HL})(\text{btc})(\text{H}_2\text{O})_{0.5}(\mathbf{5})$. In **5**, the unit cell contains one Zn(II) ion, three btc^{3-} ligands, one $[\text{HL}]^+$ unit, indicative of a partly protonated L ligand. The Zn ion is five-coordinated with four oxygen atoms from three btc^{3-} ligands, one nitrogen atom from $[\text{HL}]^+$ ligand (Figure 5a). The btc^{3-} ligands take $\mu_3:\eta^1\eta^0:\eta^1:\eta^1:\eta^0:\eta^1$ coordination mode to connect to three Zn ions, resulting in a wrinkle 2D layer (Figure 5b). Furthermore, the L ligands, where the dihedral angle between the naphthalene ring and the pyridine ring is 66.37° , 61.76° respectively, take monodentate coordination mode and act as a decoration in the exterior of the 2D layer (Figure 5c). A further insight into the structure is carried out by topology analysis, giving a 3-connected net with 4.8^2 topological symbol (Figure 5d). Notably, through N...H...O hydrogen bond between $[\text{HL}]^+$ ligands and btc^{3-} ligands {N2...H2M...O6(2.918Å, 166.90°), N3...H3M...O1(2.890Å, 159.29°), N4...H1M...O4(2.655Å, 171.00°) respectively}, a 3D supramolecular net is built, where a remarkable puncture structure is observed with the $[\text{HL}]^+$ ligand of one layer as mast to puncture into a 32-membered ring of one adjacent layer (Figure 5e).

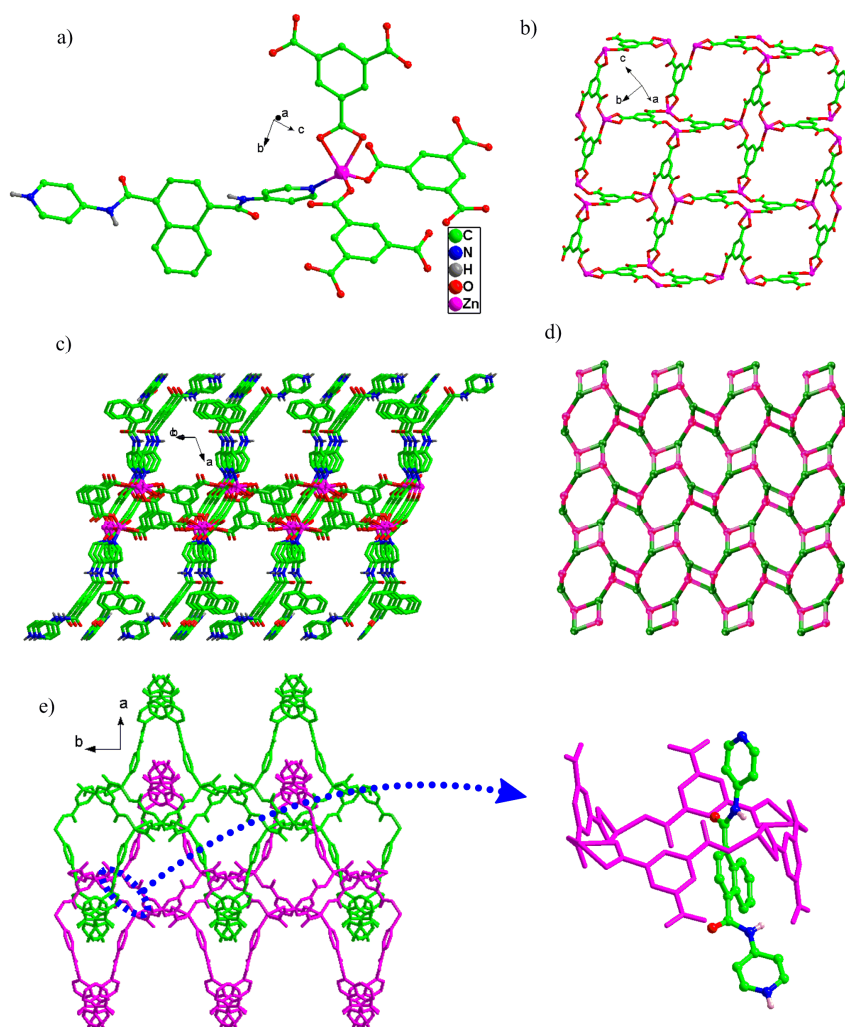


Figure 5. Structure of $\text{ZnL}(\text{btc})\cdot(\text{H}_2\text{O})_{0.5}$ (**5**). (a) Coordination environment surrounding Zn ion. (b) The view of part 2D wrinkle layer in **5**. (c) The view of 2D layer of **5**. (d) The view of the topology simplified structure of **5** (the pink/Zn nodes, the bright green/btc³⁻nodes). (e) The view of 3D puncture structure and the details of the puncture structure.

Structure of Zn(L)(nap)(6). In unit cell of **6**, there are two centrosymmetric Zn(II) ions, Zn1 and Zn1A (Symmetry code: -2-x, 2-y, -z), four nap²⁻ ligands, and two L ligands, where Zn ions linked by the carboxyl group from two nap²⁻ ligands construct a dinuclear unit, and the naphthyl of the L ligands is disordered, the dihedral angle between the naphthalene ring and the pyridine ring is 44.37°. Every Zn(II) ion is coordinated with four oxygen atoms from three different nap²⁻ ligands and one nitrogen atom from L ligand.(Figure 6a) The nap²⁻ ligands taking $\mu_3:\eta^1:\eta^1:\eta^1:\eta^1$ coordination mode link Zn ions to form a 2D layer along *ac* plane, (Figure 6b) which are further connected by the L ligands to construct a 3D pillared-layered framework. In addition, there are hydrogen bonds {N2...H1M...O3(3.060Å, 171.37°)} between the L ligands and nap²⁻ ligands, which lead to the interpenetration of the framework. Topologically, if we take the two centrosymmetric Zn ions that construct a dinuclear unit as one node, then we can obtain a 6-connected **pcu** net with (4¹².6³) topology symbol. After that, three identical **pcu** nets interpenetrate each other resulting in a 3-fold interpenetrating matrix (Figure 6c).

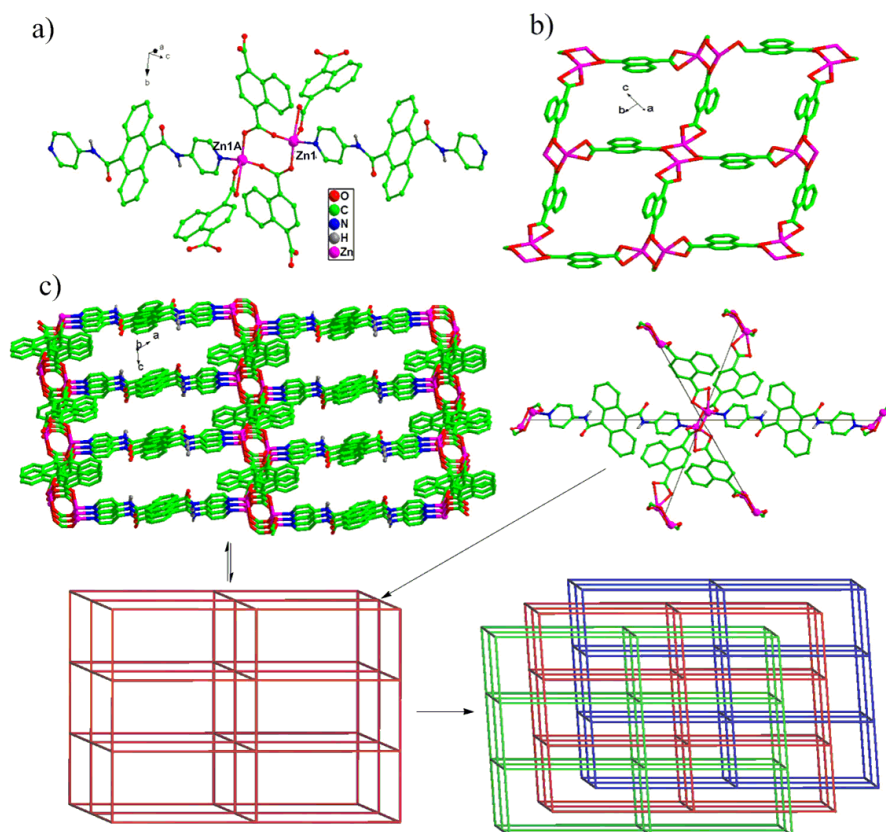


Figure 6. Structure of ZnL(nap)(6). (a) The crystal unit cell of 6. (b) The 2D layer along *ac* plane in 6. (c) The 3D pillared-layered framework of 6, the simplified cubic net with the details of nodes and the 3-fold interpenetrating nets.

Structure of Zn(L(ip)).(H₂O)₂.(CH₃CH₂OH)(7). In the unit cell of compound 7, there are two unique Zn(II) ions, Zn1 and Zn2. Zn1 is five-coordinated with three oxygen from three different ip²⁻ ligands and two nitrogen from two different L ligands where the dihedral angle between the naphthalene ring and the pyridine ring is 79.90°, 65.84° respectively. While Zn2 is six-coordinated with four oxygen atoms from three ip²⁻ ligands and two nitrogen atoms from two L ligands. (Figure 7a) In turn, the ip²⁻ ligands hold two kinds of coordination mode, $\mu_3:\eta^1:\eta^1:\eta^1:\eta^1$ and $\mu_3:\eta^1:\eta^1:\eta^1:\eta^0$. Along *a* direction, both Zn1, symmetry-related Zn1A (1-x, 1-y, 2-z) and Zn2, symmetry-related Zn2B (-1+x, y, z) are combined together by ip²⁻ ligands, creating 1D chain. Afterwards, the L ligands connect the 1D chains, forming a 2D sheet, (Figure 7b) where the hydrogen bond N2...H1M...O11(2.982Å, 166.59°) exist in the L ligands. Further through the weak interaction, the layers are extended to be 3D supramolecular framework (calculated void space using PLATON was found to be 528.8 Å³ (17.7% total of cell volume). (Figure 7c)

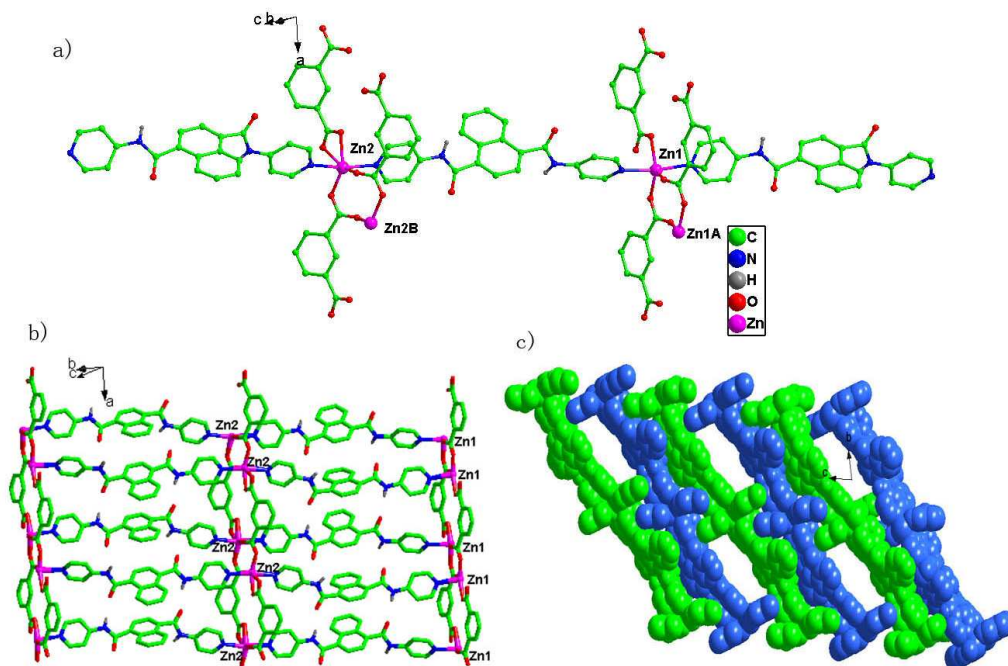


Figure 7. Structure of $\text{Zn(L)(ip).(H}_2\text{O)}_2\text{.(CH}_3\text{CH}_2\text{OH)(7)}$. (a) Coordination environment surrounding Zn ion. (b) The 2D sheet of 7. (c) The stacking 3D framework of 7.

IR ,TG and Fluorescence Properties

IR studies were carried out for compounds, **4**, **5**, **6**, **7**. The characteristic IR bands of acylamide group are observed in them (**4**: 3278, 3093, 1622; **5**: 3284, 3070, 1650; **6**: 3293, 3059, 1682; **7**: 3301, 3070, 1673 cm^{-1}), and the characteristic IR bands of carboxyl group are observed in them (**4**: 1700, 932; **5**: 1709, 935; **6**: 1733, 913; **7**: 1709, 915 cm^{-1}) are observed.

As compounds **1**, **3** show very low yield, we study the thermogravimetric and the fluorescence of the other compounds. As shown in Figure 8a, compound **2** has a continuous weight loss without any platform until 550°C indicates low thermostability of **2**, and the loss of three free H_2O molecule and three ethanol solvent existing in the large pore of the framework and one coordinated H_2O molecular (calc. 21.6%) is estimated at 30-180°C (exp. 22.2%). Compound **4** is stable to 350°C, and then has a major weight loss which is due to the chemical decomposition. In the crystal data of compound **5**, we can found it contains half free H_2O molecule, but for its small occupation, we can't find obvious weight loss between 30-350°C in the thermogravimetric curve, after that, the compound have a big weight loss which is ascribed to the chemical decomposition. Compound **6** are stable to 390°C, and then have a weight loss which due to the chemical decomposition. Compound **7** has a 9.7% weight loss between 30-250°C, which corresponds to two free H_2O molecule and one free $\text{CH}_3\text{CH}_2\text{OH}$ molecule (calc. 10.2%), then the compound begin to decompose. Further insight from this TG study gives a thermo-stability sequence, viz. **6**>**5**>**4**>**7**>**2**, and it is

possibly due to the difference of the pore structure of the 3D framework.

In Figure 8b, the compounds **2**, **5**, **6**, **7** in the solid afford strong luminescence at 399nm, 418nm, 412nm, 412nm if excited at 342nm, 367nm, 364nm, 360nm, respectively. While compound **4** has no fluorescence emission, as the L ligand is completely protonated. The excitation spectra in Figure 9b clearly give two kinds of excitation wavelength, indicative of multi-source of emission or tunable luminescence. However, further test suggests that tunable luminescence is not existent. Thus, taking into account the co-existence of L and organic carboxylate ligands, multi-source of emission is deduced. However, the similarity observed in both excitation and emission spectra for compounds **2**, **5**, **6**, **7**, indicates that the luminescence of them is mainly derived from L ligands, and the presence of other organic carboxylate ligands may generate the small difference in luminescence.

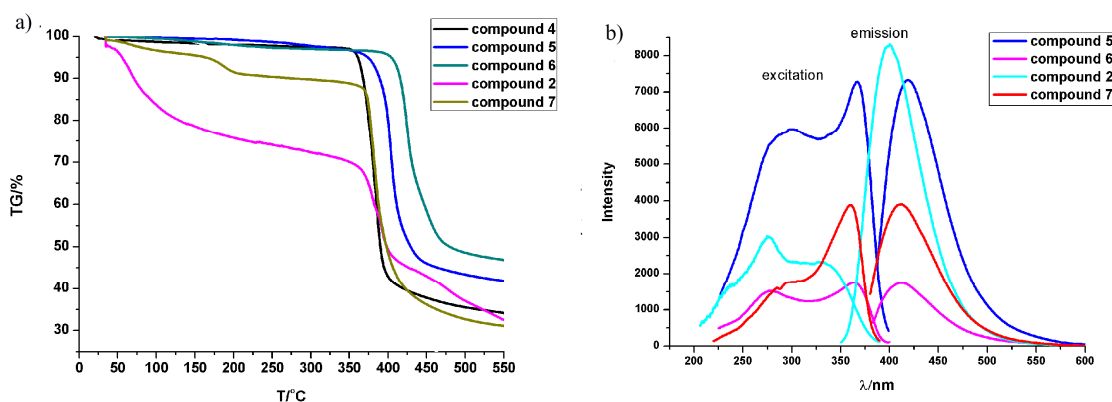


Figure 8. The TG plots, excitation and emission spectra of these acylamide-MOFs.

Conclusions

In conclusion, we represent here a series of compounds based on L ligands. With the different synthesis condition, the resulting compounds, **1-7**, show different structural features, involving interpenetrating, interlocked, puncturing, and pillared-layered framework. The results give us insight into the generating structural diversity *via* the control of reaction conditions. This work also demonstrates that L ligand is not only good coordination skeleton but also excellent supramolecule-directing template. Moreover, considerable solvent-accessible void in some compounds is also very attractive.

ACKNOWLEDGMENTS

This work was supported by the Foundation of Jiangxi Educational Committee (no. GJJ13472),

the National Natural Science Foundation of China (21203022, 21261001).

REFERENCES

- (1) (a) P. Hagrman, D. Hagrman, J. Zubieta, *Angew. Chem., Int. Ed.*, 1999, **111**, 2798; (b) Y. P. He, Y. X. Tan, J. Zhang, *Chem. Commun.*, 2013, **49**, 11323; (c) Y. P. He, Y. X. Tan, J. Zhang, *Inorg. Chem.*, 2013, **52**, 12758; (d) E. Yang, H. Y. Li, F. Wang, H. Yang, J. Zhang, *CrystEngComm.*, 2013, **15**, 658.
- (2) (a) A. Blake, N. Champness, P. Hubberstey, W. Li, M. Withersby, M. Schroder, *Coord. Chem. Rev.*, 1999, **183**, 117; (b) J. H. Cui, Y. Z. Li, Z. J. Guo, H. G. Zheng, *Chem. Commun.*, 2013, **49**, 555; (c) Z. Z. Lu, R. Zhang, Y. Z. Li, Z. J. Guo, H. G. Zheng, *J. Am. Chem. Soc.*, 2011, **133**, 4172; (d) K. Liang, H. G. Zheng, Y. L. Song, M. F. Lappert, Y. Z. Li, X. Q. Xin, Z. X. Huang, J. T. Chen, S. F. Lu, *Angew. Chem. Int. Ed.*, 2004, **43**, 5776.
- (3) (a) B. Moulton, M. Zaworotko, *Chem. Rev.*, 2001, **101**, 1629; (b) O. Evans, W. B. Lin, *Acc. Chem. Res.*, 2002, **35**, 511.
- (4) M. Yaghi, M. O'Keeffe, N. Ockwig, H. Chae, M. Eddaoudi, J. Kim, *Nature*, 2003, **423**, 705.
- (5) (a) A. Müller, S. Das, S. Talismanov, S. Roy, E. Beckmann, H. Böggge, M. Schmidtman, A. Merca, A. Berkle, L. Allouche, Y. Zhou, L. Zhang, *Angew. Chem., Int. Ed.*, 2003, **115**, 5193; (b) C. Rao, S. Natarajan, R. Vaidhyanathan, *Angew. Chem., Int. Ed.*, 2004, **116**, 1490; (c) X. M. Zhang, J. Q. Li, S. J. Liu, M. B. Luo, W. Y. Xu, F. Luo, *CrystEngComm*, 2014, **16**, 2570.
- (6) (a) P. J. Steel, *Acc. Chem. Res.*, 2005, **38**, 243; (b) S. L. James, *Chem. Soc. Rev.*, 2003, **32**, 276.
- (7) (a) M. H. Zeng, W. X. Zhang, X. Z. Sun, X. M. Chen, *Angew. Chem., Int. Ed.*, 2005, **44**, 3079; (b) M. H. Zeng, B. Wang, X. Y. Wang, W. X. Zhang, X. M. Chen, S. Gao, *Inorg. Chem.*, 2006, **45**, 7069; (c) M. H. Zeng, S. Gao, X. M. Chen, *Inorg. Chem. Commun.*, 2004, **7**, 864.
- (8) (a) M. H. Zeng, M. C. Wu, H. Liang, Y. L. Zhou, X. M. Chen, S. W. Ng, *Inorg. Chem.*, 2007, **46**, 7241; (b) M. H. Zeng, S. Gao, X. M. Chen, *New J. Chem.*, 2003, **27**, 1599; (c) Q. J. Deng, M. C. Wu, M. H. Zeng, H. J. Liang, *Mol. Struct.*, 2007, **828**, 14.
- (9) (a) P. M. Forster, N. Stock, A. K. Cheetham, *Angew. Chem., Int. Ed.*, 2005, **44**, 7608; (b) J. Ni, K. J. Wei, Y. Liu, X. C. Huang, D. Li, *Cryst. Growth Des.*, 2010, **10**, 3964; (c) G. C. Ou, X. L. Feng, T. B. Lu, *Cryst. Growth Des.*, 2011, **11**, 851; (d) A. Stephenson, S. P. Argent, T. R. Johannessen, I. S. Tidmarsh, M. D. Ward, *J. Am. Chem. Soc.*, 2011, **133**, 858.
- (10) (a) F. Luo, G. M. Sun, A. M. Zheng, S. X. Lian, Y. L. Liu, X. F. Feng, Y. Y. Chu, *Dalton Trans.*, 2012, **41**, 13280; (b) Y. Zhu, F. Luo, M. B. Luo, X. F. Feng, S. R. Batten, G. M. Sun, S. J. Liu, W. Y. Xu, *Dalton Trans.*, 2013, **42**, 8545; (c) Y. M. Song, F. Luo, M. B. Luo, Z. W. Liao, G. M. Sun, X. Z. Tian, Y. Zhu, Z. J. Yuan, S. J. Liu, W. Y. Xu, X. F. Feng, *Chem. Commun.*, 2012, **48**, 1006.

- (11) (a) G. A. Farnum, A. L. Pochodylo, R. L. LaDuca, *Cryst. Growth Des.*, 2011, **11**, 678; (b) X. F. Wang, Y. Lu, T. A. Okamura, H. Kawaguchi, G. Wu, W. Y. Sun, N. Ueyama, *Cryst. Growth Des.*, 2007, **7**, 1125; (c) J. G. Lin, S. Q. Zang, Z. F. Tian, Y. Z. Li, Y. Y. Xu, H. Z. Zhu, Q. J. Meng, *CrystEngComm*, 2007, **9**, 915.
- (12) (a) Y. Zhu, F. Luo, Y. M. Song, X. F. Feng, M. B. Luo, Z. W. Liao, G. M. Sun, X. Z. Tian, Z. Z. Yuan, *Cryst. Growth Des.*, 2012, **12**, 2158; (b) Y. M. Song, F. Luo, Y. Zhu, X. Z. Tian, G. M. Sun, *Aust. J. Chem.*, 2013, **66**, 98. (c) X. L. Wu, F. Luo, G. M. Sun, A. M. Zheng, J. Zhang, M. B. Luo, W. Y. Xu, Y. Zhu, X. M. Zhang, S. Y. Huang, *ChemPhysChem* 2013, **14**, 3594.
- (13) (a) F. Luo, S. R. Batten, *Dalton Trans.*, 2010, **39**, 4485; (b) F. Luo, M. B. Luo, Y. H. Liu, *CrystEngComm*, 2010, **12**, 1750; (c) H. X. Huang, F. Luo, G. M. Sun, Y. M. Song, X. Z. Tian, Y. Zhu, Z. Z. Yuan, X. F. Feng, M. B. Luo, *CrystEngComm*, 2012, **14**, 7861; (d) Z. Z. Yuan, F. Luo, Y. M. Song, G. M. Sun, X. Z. Tian, H. X. Huang, Y. Zhu, X. F. Feng, M. B. Luo, S. J. Liu, W. Y. Xu, *Dalton Trans.*, 2012, **41**, 12670; (e) Y. C. Qin, X. F. Feng, F. Luo, G. M. Sun, Y. M. Song, X. Z. Tian, H. X. Huang, Y. Zhu, Z. J. Yuan, M. B. Luo, S. J. Liu, W. Y. Xu, *Dalton Trans.*, 2013, **42**, 50; (f) G. M. Sun, H. X. Huang, X. Z. Tian, Y. M. Song, Y. Zhu, Z. J. Yuan, W. Y. Xu, M. B. Luo, S. J. Liu, X. F. Feng, F. Luo, *CrystEngComm*, 2012, **14**, 6182.
- (14) T. J. Jenkins, B. Guan, M. S. Dai, G. Li, T. E. Lightburn, S. Huang, B. S. Freeze, D. F. Burdi, S. Jacutin-Porte, R. Bennett, W. R. Chen, C. Minor, S. Ghosh, C. Blackburn, K. M. Gigstad, M. Jones, R. Kolbeck, W. Yin, S. Smith, D. Cardillo, T. D. Ocain, G. C. Harriman, *J. Med. Chem.*, 2007, **50**, 566.
- (15) D. Moffat, S. Patel, F. Day, A. Belfield, A. Donald, M. Rowlands, J. Wibawa, D. Brotherton, L. Stimson, V. Clark, J. Owen, L. Bawden, G. Box, E. Bone, P. Mortenson, A. Hardcastle, S. V. Meurs, S. Eccles, F. Raynaud, W. Aherne, *J. Med. Chem.*, 2010, **53**, 8663.
- (16) Y. Niko, Y. Hiroshige, S. Kawauchi, G. Konishi, *J. Org. Chem.*, 2012, **77**, 3986.
- (17) (a) J. Fan, B. E. Hanson, *Inorg. Chem.*, 2005, **44**, 6998; (b) G. C. Xu, Q. Hua, T.-a. Okamura, Z. S. Bai, Y. J. Ding, Y. Q. Huang, G. X. Liu, W. Y. Sun, N. Ueyama, *CrystEngComm*, 2009, **11**, 261.
- (18) (a) J. F. Eubank, R. D. Walsh, P. Poddar, H. Srikanth, R. W. Larsen, M. Eddaoudi, *Cryst. Growth Des.*, 2006, **6**, 1453; (b) L. N. Jia, L. Hou, L. Wei, X. J. Jing, B. Liu, Y. Y. Wang, Q. Z. Shi, *Cryst. Growth Des.*, 2013, **13**, 1570; (c) A. M. P. Peedikakkal, J. J. Vittal, *Cryst. Growth Des.*, 2011, **11**, 4697. (d) K. L. Huang, X. Liu, J. K. Li, Y. W. Ding, X. Chen, M. X. Zhang, *Cryst. Growth Des.*, 2010, **10**, 1508.